



OPEN

Ovulation and extra-ovarian origin of ovarian cancer

SUBJECT AREAS:

CANCER MODELS
CANCERYang Yang-Hartwich¹, Marta Gurrea-Soteras¹, Natalia Sumi¹, Won Duk Joo², Jennie C. Holmberg¹, Vinicius Craveiro¹, Ayesha B. Alvero¹ & Gil Mor¹Received
14 May 2014Accepted
25 July 2014Published
19 August 2014Correspondence and
requests for materials
should be addressed to
G.M. (gil.mor@yale.
edu)¹Department of Obstetrics and Gynecology, Yale University School of Medicine, New Haven, CT 06520, USA, ²CHA Bundang Medical Center, CHA University, South Korea.

The mortality rate of ovarian cancer remains high due to late diagnosis and recurrence. A fundamental step toward improving detection and treatment of this lethal disease is to understand its origin. A growing number of studies have revealed that ovarian cancer can develop from multiple extra-ovarian origins, including fallopian tube, gastrointestinal tract, cervix and endometriosis. However, the mechanism leading to their ovarian localization is not understood. We utilized *in vitro*, *ex vivo*, and *in vivo* models to recapitulate the process of extra-ovarian malignant cells migrating to the ovaries and forming tumors. We provided experimental evidence to support that ovulation, by disrupting the ovarian surface epithelium and releasing chemokines/cytokines, promotes the migration and adhesion of malignant cells to the ovary. We identified the granulosa cell-secreted SDF-1 as a main chemoattractant that recruits malignant cells towards the ovary. Our findings revealed a potential molecular mechanism of how the extra-ovarian cells can be attracted by the ovary, migrate to and form tumors in the ovary. Our data also supports the association between increased ovulation and the risk of ovarian cancer. Understanding this association will lead us to the development of more specific markers for early detection and better prevention strategies.

Ovarian cancer is the most lethal gynecologic malignancy and will cause an estimated 14,030 deaths in 2014 in the United States¹. The majority of ovarian cancer patients are diagnosed at advanced stage when tumors have metastasized. Substantial efforts have been undertaken to develop early detection tests in order to improve the prognosis and survival rate of ovarian cancer. However, these efforts are hindered by our limited knowledge about the origin of ovarian cancer.

Recent studies have revealed that ovarian cancer is a complex disease that develops from multiple extra-ovarian origins. First, ovarian cancer encompasses several histologically and molecularly distinct malignancies in the ovaries, including serous, mucinous, endometrioid, and clear cell carcinomas. Second, each of these distinct subtypes has been traced back to independent cell origins outside the ovary. In the case of high-grade serous ovarian cancer (HGSOC), an increasing number of studies support the hypothesis that fallopian tube epithelial cells are the origin of HGSOC. This theory is supported by the evidence that pre-malignant precursor lesions labeled by the “p53 signature”, a benign-appearing population of cells harboring DNA damage and p53 mutations, have been found in the fallopian tubes^{2,3}. In addition, serous tubal intra-epithelial carcinoma in the distal end of the fallopian tubes have been observed in 5–10% of women with BRCA mutations who underwent prophylactic salpingo-oophorectomy^{4,5}. Moreover, non-neoplastic fallopian tube epithelial cells and serous ovarian carcinoma share similar morphologic and immunophenotypic features⁶. The origins of mucinous ovarian tumors are postulated to be metastatic tumors from the gastrointestinal tract or cervix^{7,8}. For clear cell and endometrioid ovarian cancers, they are considered to originate from endometriosis. The studies that have uncovered the extra-ovarian origins help us understand why salpingectomy and hysterectomy can reduce the risk of ovarian cancer⁹.

One of the main questions to arise is why these extra-ovarian malignant cells from diverse origins all establish solid tumors in the ovary. The answer may lie in the unique functional characteristics of the ovaries. During ovulation, the ovary releases one egg through the rupture of ovarian follicle. The rupture and repair process during menstrual cycles repeatedly creates a local inflammatory microenvironment in which cytokines and growth factors are produced at the ovulatory wound site of the ovary¹⁰. Therefore, the ovary is a plausible source of chemotactic factors that can recruit extra-ovarian pre-malignant and malignant cells. Within the ovary, the post-ovulatory inflammatory and pro-repair environment can provide tumorigenic factors that support malignant transformation or maintain malignant cell survival. This may explain why increased ovulation is a risk factor



of ovarian cancer and why the inhibitory factors of ovulation such as multiple pregnancies, breastfeeding, late menarche, and the use of oral contraceptives, reduce ovarian cancer risk according to the epidemiological studies^{11,12}.

In this study, we sought to identify the key factors and related pathways that can promote the extra-ovarian malignant cells to establish tumors in the ovaries. We developed xenograft mouse models that can closely mimic ovarian cancer at different stages and showed that the ovulatory wound promotes the cellular migration of transformed cells to the ovary and their establishment as tumors in the ovary. Using this model, we identified the granulosa cell secreted SDF-1 and collagen IV as key factors that are able to attract and maintain malignant cells in the ovaries and promote tumorigenesis. These factors are present and exposed particularly during ovulation and therefore support the specific association between ovulation and ovarian tumorigenesis.

Results

Superovulation promotes ovarian tumor formation. Our group previously reported a population of CD44⁺/MyD88⁺ ovarian cancer cells that had tumor initiating capacity¹³. To monitor the tumor formation of these ovarian tumor-initiating cells (OTICs), we labeled them with mCherry-expressing lentivirus. The mCherry-labeled OTICs (mCherry-OTICs) were injected intraperitoneally (i.p.) in nude mice and developed into extensive carcinomatosis, mostly in areas rich in fat such as the omentum, diaphragm, and peritoneum (Fig. 1Aa). These OTICs were so aggressive that all the animals developed intraperitoneal carcinomatosis. More important, 15 out of 39 mice that were injected with mCherry-OTICs developed tumors in the ovaries (Fig. 1A and 1B). To test the hypothesis that ovulation may influence the formation of ovarian tumors, 24 mice were superovulated after i.p injection of mCherry-OTICs. All the mice in the superovulation group were found to bear tumors in their ovaries (Fig. 1B), suggesting that ovulation can enhance the homing and establishment of malignant cells in the ovaries.

Intrauterine injection of OTICs forms in situ ovarian cancer. To study the early establishment of malignant cells in the ovaries, we modified our model by delivering mCherry-OTICs through intrauterine injection. The mCherry-OTICs were injected into the distal part of one uterine horn (Fig. 2A), which confined OTICs to the reproductive tract and allowed us to mimic the migration of

malignant cells from fallopian tubes, uterus or cervix towards ovaries. Superovulation was induced after the intrauterine injection. Four days after injection, most of the mCherry-OTICs localized in the uterine horn (Fig. 2B). Around day 5 to day 7, there were increasing numbers of mCherry-OTICs that attached to the ovaries and surrounding adipose tissue (Fig. 2B). By in vivo imaging the fluorescence of mCherry-OTICs we detected tumors at the approximate anatomical location of the ovaries as early as 5 days post-injection (Fig. 2C). About 12 days post-injection a significantly stronger fluorescent signal usually appeared at the same location, confirming the establishment of tumors in the ovaries (Fig. 2C). The necropsy of these mice confirmed that mCherry positive tumors protruded from the surface of the ovary (Fig. 2D).

To study the early establishment of these ovarian tumors, we examined the tumor development at different stages by sectioning and staining these mouse ovaries. Five days after the injection of mCherry-OTICs, small groups of cancer cells attached to the areas with apparent disrupted surface epithelium of the ovaries (Fig. 3A). Cancer cells were often localized in the areas adjacent to the corpus luteum (Fig. 3B). Ten days after injection, cancer cells could be observed within mouse ovarian stroma. The single layer of mouse ovarian surface epithelium, which enclosed tumors inside the ovary (Fig 3C–D), was intact. We used immunofluorescence staining for mouse cytokeratin 8 (CK8, an epithelial marker) to confirm the presence of mouse epithelial cells surrounding the mCherry-expressing xenograft ovarian tumors (Fig. 3G–I). This histological feature of a covering layer of surface ovarian epithelial cells is also often observed in human ovarian tumors. At this early stage, we observed cancer cells only within the ovaries on the side of injection. The mass of cancer cells continued proliferating within the stroma of the ovaries until day 25–30 post-injection, when we could observe the tumor protruding from the ovarian surface (Fig. 3E–F). After 30 days, the majority of the mice developed metastatic tumors in the peritoneal cavity; furthermore, fifty percent of the mice showed ovarian tumors in the contralateral ovary. These findings demonstrated that the extra-ovarian malignant cells ascending from the uterus could form in situ ovarian tumors and further advance to metastatic tumors. The observation that cancer cells were present in close proximity to the corpus luteum suggested its possible role in the process of tumorigenesis and may explain the increase in ovarian tumors observed in superovulated mice.

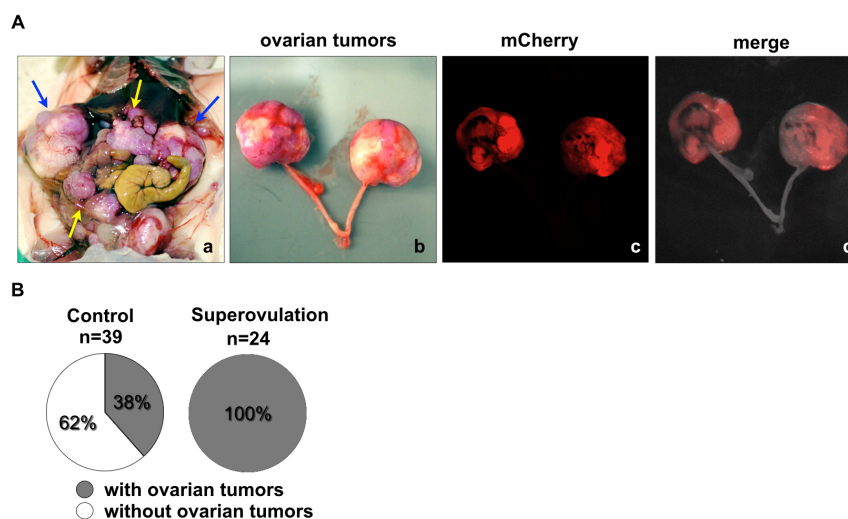


Figure 1 | Superovulation promotes ovarian tumor formation. (A). Representative images of tumors formed by intraperitoneally injected mCherry-OTICs. a. Interperitoneal tumors (yellow arrows) and ovarian tumors (blue arrows). b–d. Ovaries with tumors formed by mCherry-OTICs. (B). Pie graphs indicate the percentage of mice with ovarian tumors.

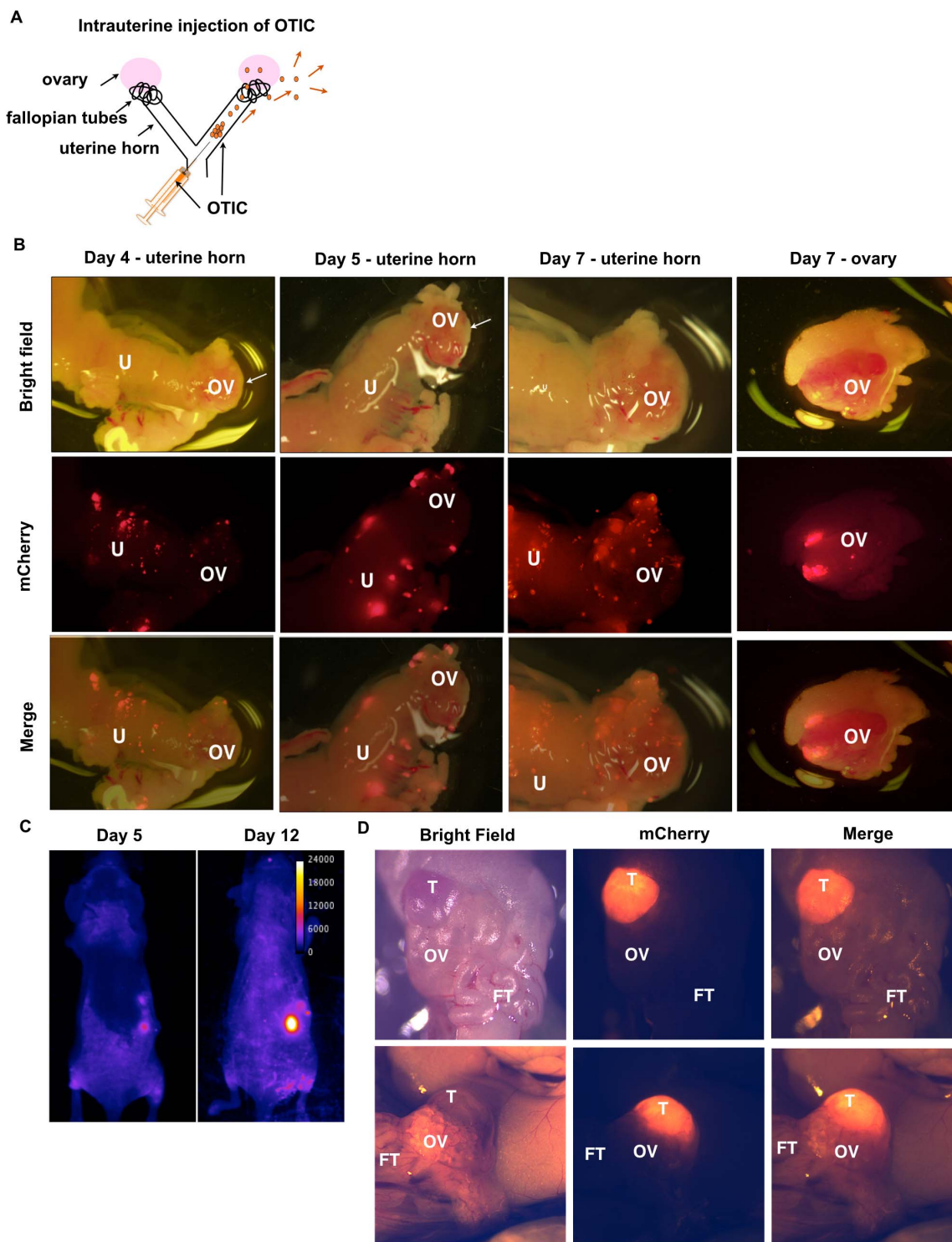


Figure 2 | The intrauterine injections of mCherry-OTICs form ovarian tumors. (A). A diagram illustrates the intrauterine injection of OTICs. (B). Representative images of mouse partial uterus horn and ovary after intrauterine injection of mCherry-OTICs. (C). In vivo live imaging of mouse with ovarian tumor formed by mCherry-OTICs. (D). Ovarian tumors examined with Fluorescent Stereo Microscope. (U, uterus horn. OV, ovary. FT, fallopian tubes. T, tumor.)

Granulosa cell secreted SDF-1 attracts tumor initiating cells.

Ovulation is characterized by the production of cytokines and chemokines. The role of these cytokines and chemokines includes follicle rupture and remodeling, immune cell infiltration, angiogenesis and oocyte maturation¹⁴. It is conceivable that these factors may also act as a chemoattractant to malignant cells.

Toward the goal of identifying ovulation-associated specific molecules and pathways that promote the establishment of tumors in the ovary, we first identified the cytokines that were upregulated during ovulation. We compared the cytokine expression of ovaries from superovulated and control mice and detected significantly higher levels of SDF-1 (stromal cell-derived factor 1, also known as

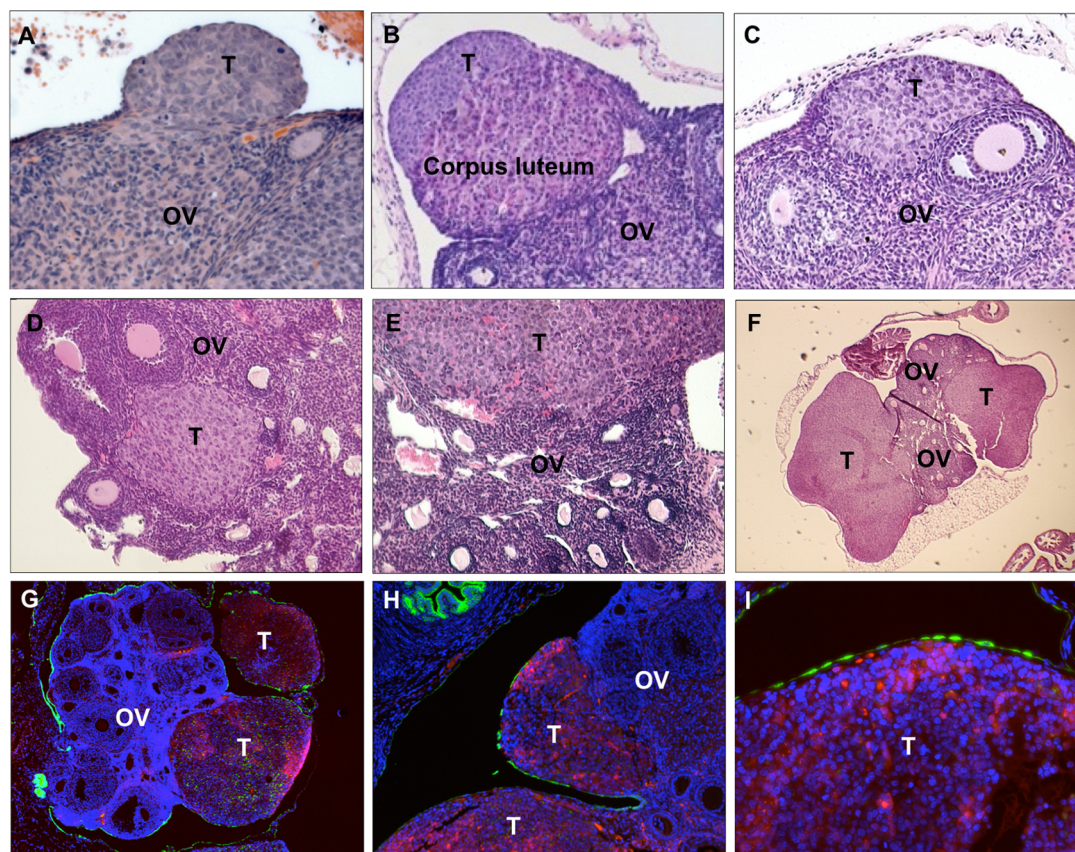


Figure 3 | Intrauterine injection of OTICs forms in situ ovarian cancer in superovulated mice. (A–F). H&E staining of mouse ovaries with tumors formed by OTICs. (G–I). Immunofluorescence staining of mouse ovaries with mCherry tumors. (Green, CK8. Red, mCherry. Blue, DAPI. OV, ovary. FT, fallopian tubes. T, tumor.)

C-X-C motif chemokine 12, CXCL12), TGF- β 2 (transforming growth factor- β 2), IL-6 (interleukin-6), and EGF (epidermal growth factor) in the ovaries of superovulated mice (Fig. 4A).

SDF-1 regulates a variety of physiological processes including spermatozoa chemotaxis, the trafficking of other tissue/organ specific stem/progenitor cells and haemato/lymphopoietic cells, and the migration of embryonic germ cells to the gonads^{15–17}. The receptor for SDF-1, CXCR4, is expressed in ovarian tumors and ovarian cancer cell lines and has been previously associated with ovarian cancer progression^{18,19}. Immunohistochemistry analysis showed high levels of SDF-1 in the follicular fluid and in the granulosa cells of mature follicles (Fig. 4Ba–e) as well as in the granulosa lutein cells in the corpus luteum (Fig. 4Bf). To determine if the SDF-1/CXCR4 interaction plays a relevant role in the migration of mCherry-OTICs to ovary, we performed in vitro migration assay (Fig. 4C–D). The migration of mCherry-OTICs was enhanced by the conditional media from a luteinized KGN cell line, which is a human steroidogenic ovarian granulosa-like tumor cell line²⁰. Adding an SDF-1/CXCR4 inhibitor, AMD3100, to the conditional media of KGN cells repressed the migration of mCherry-OTICs (Fig. 4C–D). KGN cells have many features of normal granulosa cells. They are luteinized by luteinizing hormone (LH), which can be used to study the molecular phenotype of granulosa cells during ovulation. The result that mCherry-OTICs were attracted to the condition media of KGN cells suggested that ovarian granulosa cells-secreted factors are able to induce the migration of malignant cells towards the ovary. More important, the inhibition of migration by AMD3100 demonstrated that the granulosa cell-secreted SDF-1 was critical for attracting these malignant cells.

The interaction of SDF-1 and CXCR4 activates diverse downstream signaling pathways that can result in chemotaxis, cell proliferation and survival, migration and gene transcription. Many of the effects induced by CXCR4 depend on ERK (extracellular signal-regulated kinase/mitogen-activated protein kinase) activation²¹. In mCherry-OTICs cells, the ERK pathway was activated by the condition media of luteinized KGN cells as shown by the upregulation of phosphorylated ERK (pERK) (Fig. 4E). The activation of ERK was abrogated when AMD3100 was added to the condition media (Fig. 4E), which further confirmed that SDF-1/CXCR4 interaction was critical for attracting the migration of malignant cells. Collectively, our data suggested that granulosa cell-secreted SDF-1, which is upregulated during ovulation, induced the migration of malignant cells to the ovary.

TNF α enhances SDF-1 induced migration of OTICs. Besides SDF-1, many other pro-inflammatory cytokines are produced in the unique microenvironment associated with ovulation. We postulate that the crosstalk signaling between these factors may also promote the migration of malignant cells towards the ovary. TNF α (tumor necrosis factor α) is a pro-inflammatory cytokine that plays a central role in regulating ovulation²². It is produced in the follicle to mediate follicle weakening and ovarian rupture²³. We tested whether TNF- α could enhance the migration OTICs.

Quantitative RT-PCR data showed that when OTICs were treated with TNF α (10 ng/ml) the levels of CXCR4 mRNA were significantly increased in a time-dependent manner (Fig. 5A). These findings were confirmed at the protein level by flow cytometry analysis. We observed an increase of CXCR4 expression on the surface OTICs treated with TNF α (Fig. 5B). Next, we examined through increasing

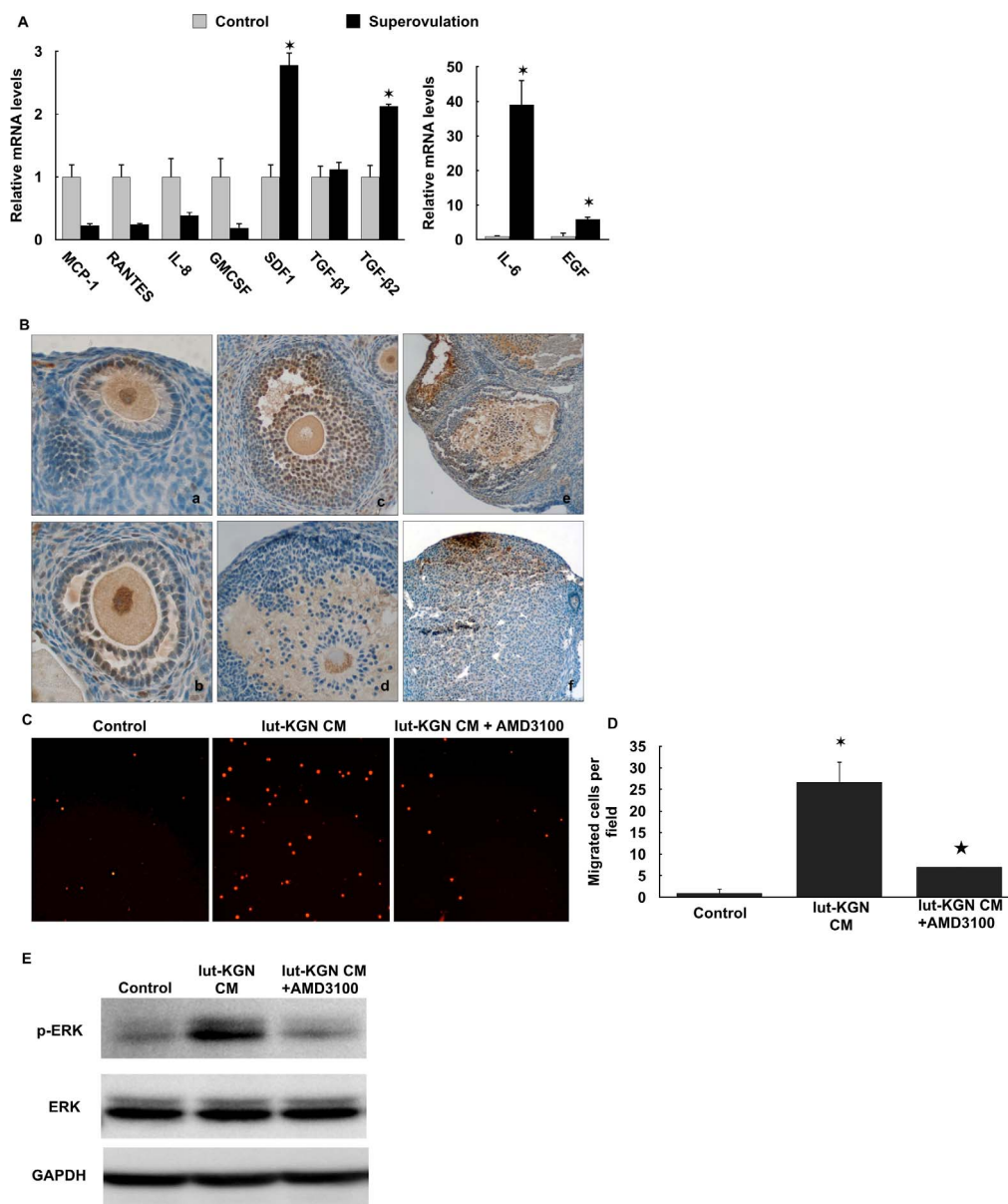


Figure 4 | Ovary-secreted SDF-1 promotes the migration of OTICs. (A). Quantitative RT-PCR of chemokines, cytokines, and growth factors in mouse ovaries. * $P < 0.05$ vs the control ovaries ($n = 3$). (B). IHC staining of SDF-1 in mouse ovary. (Brown, SDF-1. Blue, nuclei). (C). Images of mCherry-OTICs that migrated to the lower chamber in migration assay. (D). Quantification of migrated mCherry-OTICs. * $P < 0.05$ vs control group vs ★ $P < 0.05$ vs Lut-KGN CM group. (E). Western blots of p-ERK and total ERK in OTICs. GAPDH was used as loading control. The full-length blots are included in supplementary information. (Lut-KGN CM, luteinized KGN cell conditional medium. AMD3100, an SDF-1/CXCR4 inhibitor.)

CXCR4 expression whether $\text{TNF}\alpha$ enhanced the downstream signaling of SDF-1. The Western Blot result showed that $\text{TNF}\alpha$ treatment further upregulated SDF-1 induced pERK in OTICs; this effect was blocked by the addition of CXCR4 inhibitor AMD3100 (Fig. 5C). This result confirmed that the effect of $\text{TNF}\alpha$ is specific to SDF-1/CXCR4 signaling.

In addition, using in vitro scratch assay we demonstrated that as a result of enhancing the SDF-1/CXCR4 signaling $\text{TNF}\alpha$ promoted the migration of OTICs. The time-lapse imaging (Fig. 5D) and wound width quantification (Fig. 5E) analysis demonstrated that SDF-1 accelerated the migration of OTICs and shortened the time to fill the scratching wounds. When OTICs were pre-treated with $\text{TNF}\alpha$ and then treated with SDF-1, their migration was further enhanced. Taken together, our data suggested that within the pro-inflammatory microenvironment created as result of ovulation, $\text{TNF}\alpha$ increased the expression of CXCR4 in malignant cells, which made these cells

more sensitive to the signals induced by SDF-1 and promoted their migration to the ovary.

Ovarian stroma provides a scaffold for the adhesion of extra-ovarian malignant cells. The rupture of surface epithelium is a distinguishing characteristic of the ovary during ovulation. The rupture exposes the underlying ovarian stroma. The stromal cells secrete extracellular matrix (ECM), provide structural support to the follicle and maintain cellular organization and connectivity within the ovary. ECM also plays a prominent role in ovarian function by regulating the processes of cell adhesion, migration, proliferation, and differentiation^{24,25}. We hypothesized that the exposure of stromal ECM upon ovulation may create an access for extra-ovarian malignant cells to home in the ovary. Furthermore, it is plausible that the ovarian stroma provides the optimal ECM scaffold for the extra-ovarian malignant cells to adhere. Thus, the ovulation-

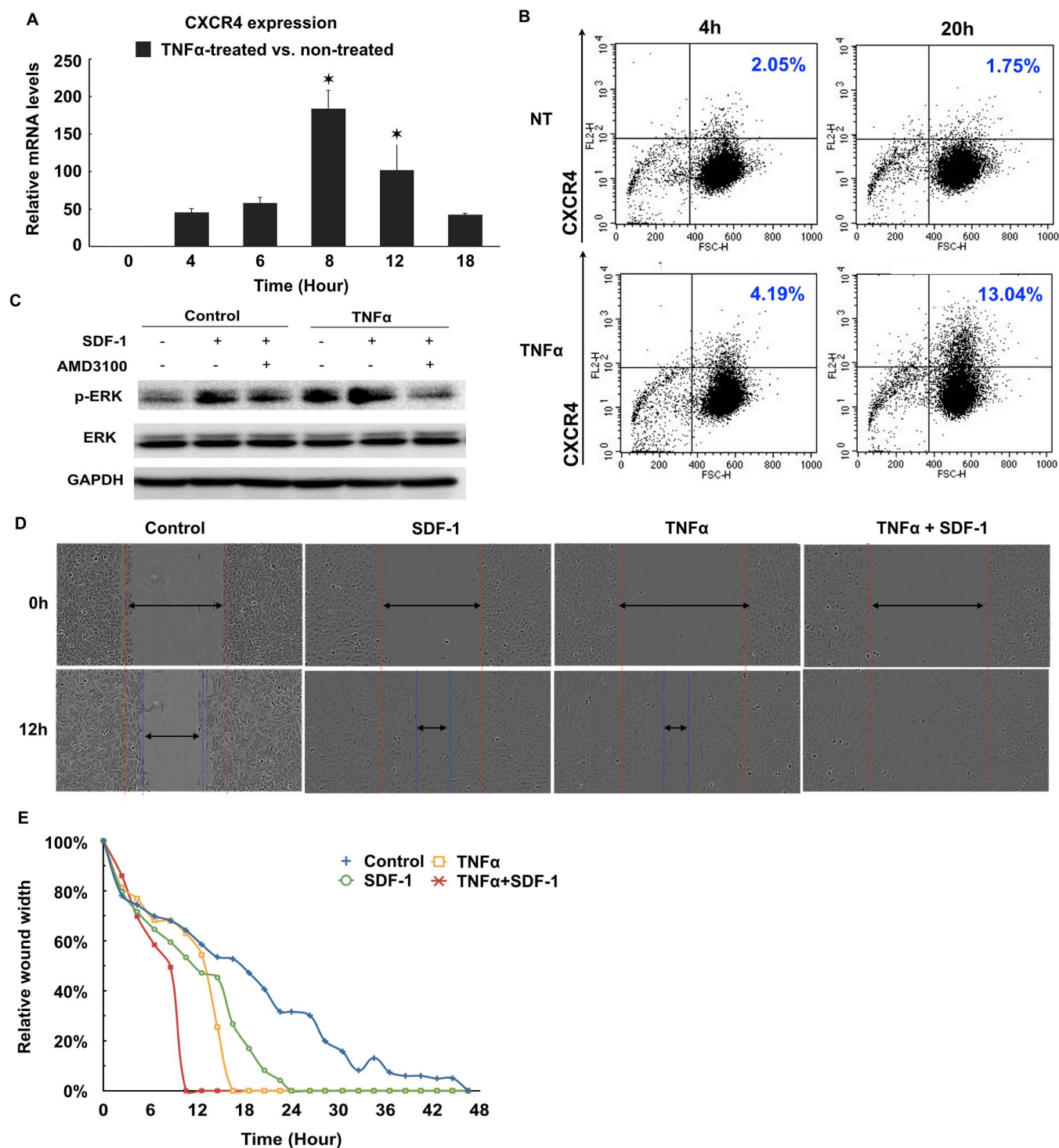


Figure 5 | **TNF α enhances the SDF-1/CXCR4 signaling in OTICs.** (A). Quantitative RT-PCR of CXCR4 in OTICs treated with TNF α . *P<0.05 vs control. (B). Flowcytometry analysis of cell surface CXCR4. Non-treated (NT) and TNF α -treated (TNF α) OTICs were stained with Alexa Fluor 594-labeled anti-CXCR4 antibody (FL2) and analyzed at 4 h and 20 h. The percentage of cells expressing high levels of CXCR4 was indicated in the graphs. (C). Western blots of p-ERK and total ERK in OTICs. GAPDH was used as loading control. The full-length blots are included in supplementary information. (D). Images of wound healing assay. (E). Wound width-time dependent curves for wound healing assay of OTICs.

induced exposure of ovarian stroma might facilitate the development of ovarian tumors.

To test this hypothesis, we first isolated mouse ovarian stromal (mOST) and mouse ovarian surface epithelial (mOSE) cells. The purity of the culture was confirmed by staining the cells with stromal cell marker vimentin and epithelial cell marker CK8 (cytokeratin 8). The mOST cells are vimentin+/CK8-, while the mOSE cells are

vimentin-/CK8+ (Fig. 6A). Cells were cultured as monolayers to produce and deposit ECM for 5 days before the GFP-labeled OTICs were seeded. GFP-OTICs adhered to mOST cells; they spread and became flattened about 1 hour after seeded. In contrast, FITC-OTICs did not adhere to mOSE cells (Fig. 6B) and remained rounded and floating in the supernatant even after 48 h post seeding. This observation suggests that malignant cells adhere to ovarian stroma



better than to the intact surface epithelium. Since the ovarian stroma is exposed only when the surface epithelium ruptures during ovulation, it further suggests that ovulation may allow the adhesion of extra-ovarian malignant cells to the ovary.

To identify the ECM components that bind to OTICs, we compared the ECM products secreted by mOST and mOSE cells. Quantitative RTPCR data showed that collagen IV and tenascin C mRNA levels were significantly higher in mOST cells compared to mOSE cells (Fig. 7A). Since integrins are the receptors that mediate the adhesion of cells to ECM, we evaluated the expression of integrins in OTICs. We compared OTICs to CD44-/MyD88- ovarian cancer cells that lack tumor-initiating capacity. Interestingly, we observed that OTICs expressed higher levels of integrin $\alpha 1$, $\alpha 2$, $\beta 1$ and $\beta 6$ mRNA than non-TICs (Fig. 7B). It is important to note that integrins $\alpha 1\beta 1$ and $\alpha 2\beta 1$ are the receptors for collagen IV and integrin $\alpha v\beta 6$ is the receptor for tenascin C^{26–28}, both of which are highly expressed in the ovarian stroma (Fig. 7A).

We confirmed the enrichment of collagen IV in the stroma of early and late corpus lutea of mouse ovaries by IHC staining (Fig. 7C). By contrast, the ovarian surface epithelium expressed very low levels of collagen IV. Interestingly, we observed a similar pattern in the mouse uterus. The uterine stroma cells are positive for collagen IV staining; the columnar epithelium that lines the lumen of the uterine cavity is negative (Fig. 7Cd). In our model, we rarely observed OTICs attaching to the uterus. However, if we mechanically ruptured the columnar epithelium prior to the injection of OTICs, tumors developed in the uterus (data not shown). Taken together, these results demonstrated that the rupture of the ovarian surface epithelium could contribute to the establishment of ovarian tumors from extra-ovarian origin by exposing the ovarian stroma ECM.

We further confirmed these findings with human cell lines. *In vitro* adhesion assay was performed using the ECM extracted from human ovarian stromal (hOST) cells and human ovarian surface epithelial (hOSE) cells. The results demonstrated that mcherry-OTICs adhered better to the ECM derived from hOST cells than to the ECM derived from hOSE cells (Fig. 7D–E). We also observed that significant numbers of mcherry-OTICs adhered to the collagen IV-coated surface, which again confirmed that the collagen IV enriched scaffold of ovarian stroma could provide support for the adhesion of malignant cells (Fig. 7D–E). Collectively these results indicated that ECM secreted by ovarian stroma could provide a scaffold for the extra-ovarian malignant cells to adhere. Therefore, by causing the exposure of ovarian stroma ovulation may promote the adhesion of malignant cells to the ovary.

Blocking “attraction” or “stromal scaffold” inhibits cancer cell adhesion to ovary. To further support our hypothesis, we established an *ex vivo* organ culture model, in which mouse ovaries were co-cultured with mCherry-OTICs to test the adhesion of cancer cells to the ovary. In order to control the ovulation cycle, HCG was injected into the mice 48 hours after PMS injection. We observed the maturation of follicles in mouse ovaries 19 hours after the injection of PMS (Fig. 8Aa). HCG triggered the rupture of follicles. Therefore, at 19 hours post-injection of HCG (67 hours after PMS injection) we observed the ovulation-associated blood flow increase in the ovary and multiple ovulating or ruptured follicles (Fig. 8Ab–c). Twenty-four hours after co-culture of the ovaries and cancer cells, we observed that the mCherry-OTICs specifically adhered to the areas where the ruptured follicles were located (Fig. 8B). In the ovaries that were isolated 19 hours after PMS

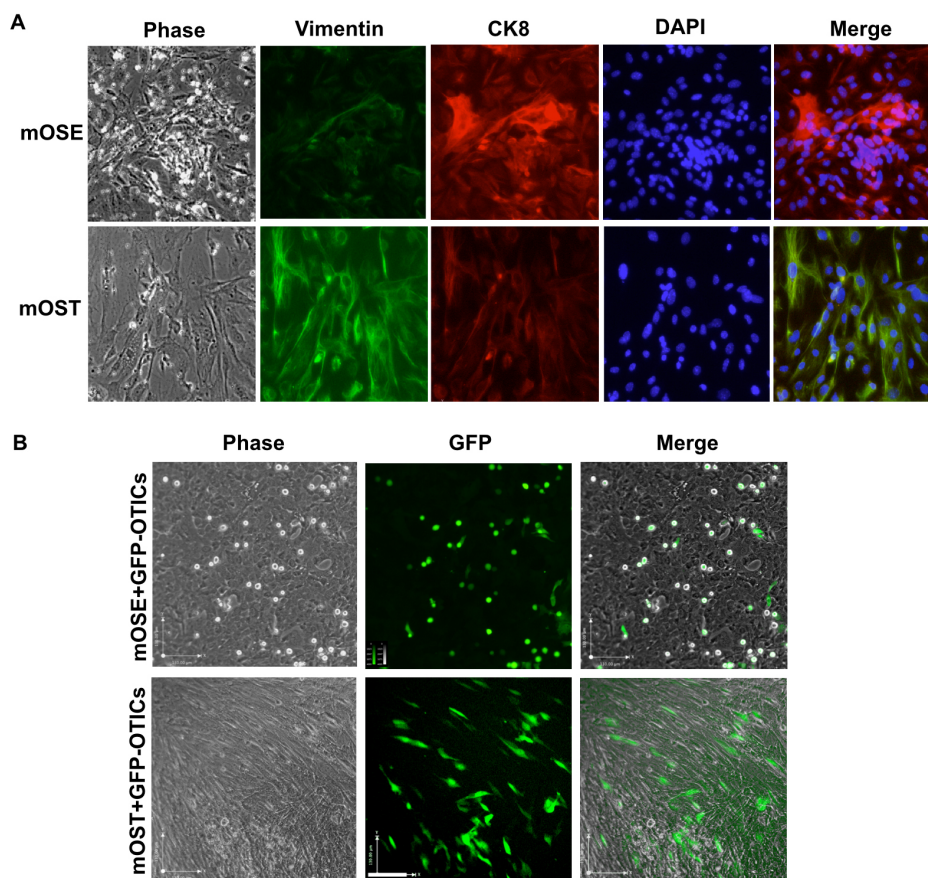


Figure 6 | OTICs adhere to ovarian stromal cells. (A). Immunofluorescence staining of mouse ovarian surface epithelial (mOSE) and mouse ovarian stromal (mOST) cells. (Green, vimentin. Red, CK8. Blue, DAPI). (B). Images of the adhesion of GFP-OTICs to mOSE and mOST cells.

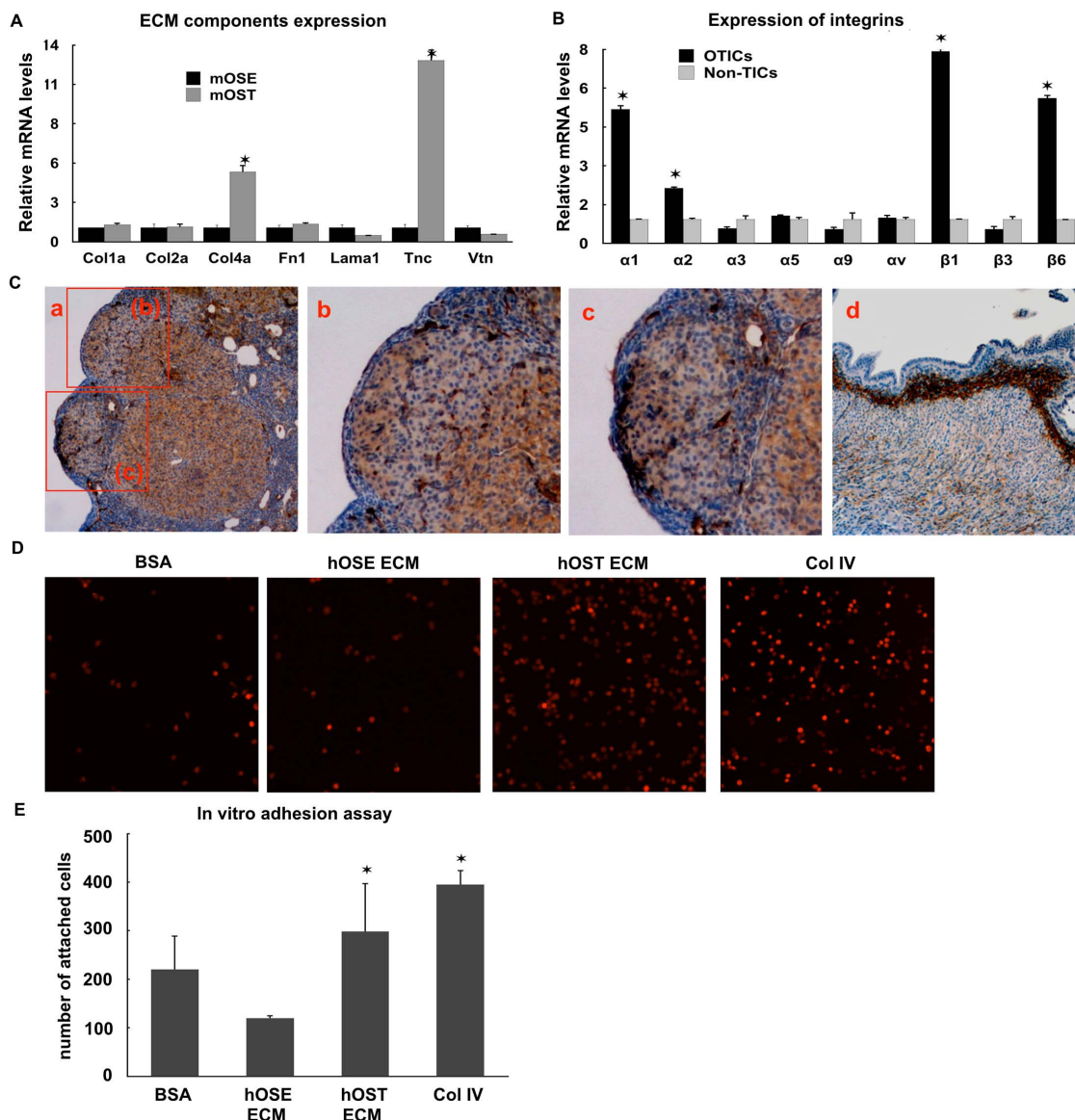


Figure 7 | Ovarian stroma provides collagen IV-enriched scaffold for the adhesion of OTICs. (A). Quantitative RT-PCR of ECM components. * $P < 0.05$ vs mOSE cells. (B). Quantitative RT-PCR of integrins. * $P < 0.05$ vs Non-TICs. (C). IHC staining of collagen IV in mouse ovary and uterus. (Brown, collagen IV. Blue, nuclei). a. mouse ovary. b–c, the enlarged images of two areas (b) and (c) in a. d. uterus. (D). Images of mCherry-OTICs that attached to the surface coated with bovine serum albumin (BSA), human ovarian surface epithelial cell-derived extracellular matrix (hOSE ECM), human ovarian stromal cell-derived extracellular matrix (hOST ECM), and collagen IV (Col IV). (E). Quantification of attached mCherry-OTICs in adhesion assay. * $P < 0.05$ vs hOSE ECM group.

injection, the adhesion of mCherry-OTICs was significantly reduced without the follicular rupture triggered by HCG (Fig 8C), suggesting that the exposure of stromal scaffold by follicular rupture is required for the adhesion of cancer cells. When ADM3100 was added to the co-culture, the adhesion of mCherry-OTICs to the ruptured follicles was significantly inhibited (Fig 8C–D). This result demonstrated that blocking the ovary-secreted SDF-1 with AMD3100 could inhibit the migration and adhesion of OTICs to the ovary. Taken together, lacking the exposure of ovarian stroma or blocking the SDF-1 attraction of OTICs towards the ovary upon ovulation could inhibit the formation of ovarian tumors (Figure 8E).

Discussion

We have described in vitro, ex vivo, and in vivo models that recapitulate the process of extra-ovarian malignant cells establishing tumors in the ovary. We have provided experimental evidence to support that by disrupting the ovarian surface epithelium and releas-

ing chemokines/cytokines, ovulation promotes the migration and adhesion of malignant cells to the ovary. Our data demonstrate that transformed cells from outside the ovary can travel to the ovary establishing tumors presenting the characteristics observed in early-stage ovarian cancer within the stroma of the ovary. We identified SDF-1 and the exposure of collagen IV-enriched ovarian stroma as the ovulation-associated factors that can contribute to ovarian tumor formation (see model in Figure 8E). Our results reveal new molecular mechanisms behind the well-known epidemiological association of ovarian cancer risk and ovulation.

The dogma that ovarian surface epithelium is the source of ovarian cancer has been challenged by new evidence. Extra-ovarian sources, such as the fallopian tubes, have been proposed as the origin of ovarian cancer. Clinical pathological studies and animal models have provided compelling evidence that the fallopian tube is a conspicuous source of high-grade serous carcinoma precursors^{6,29–33}. However, none of the studies have investigated how the cancer pre-

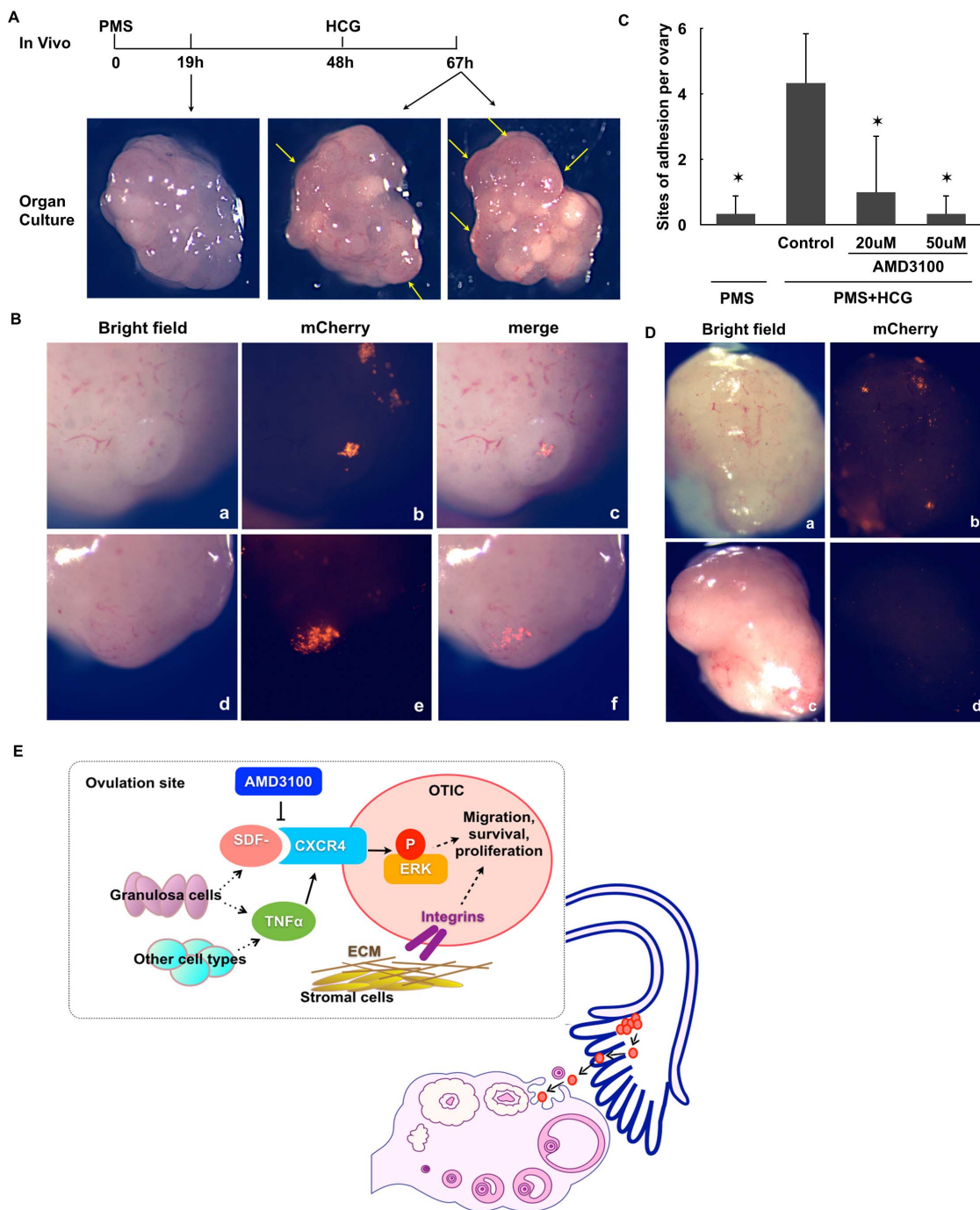


Figure 8 | Ovulation is associated with ovarian tumor formation. (A). Images of mouse ovaries. 19 hours after injecting PMS, the ovaries contain many mature follicles (a). 48 hours after injecting PMS, HCG was injected to trigger ovulation. 19 hours after injecting HCG, the ovaries contain many ovulating follicles (b, yellow arrows). (B). Images of mCherry-OTICs attaching to the ovulatory sites after 24-hour co-culture with mouse ovaries. (a, d, ovulatory sites; b, e, mCherry-OTICs; c, f, merged images.) (C). Numbers of the mCherry-OTIC adhesion sites on mouse ovaries. The numbers were counted as sites of adhesion per ovary. (PMS, ovaries 19 hours after PMS injection. PMS+HCG, 19 hours after HCG injection. Control, co-culture without AMD3100. AMD3100, co-culture with AMD3100 (20 μ M or 50 μ M) in the medium. $n=3$. * $P<0.05$ vs PMS+HCG control group) (D). AMD3100 inhibited the adhesion of mCherry-OTICs to the ovary. (a, b, control; c, d, AMD3100-treated.) (E). Schematic model of the attraction and adhesion of extra-ovarian cancer cells to the ovary.

cursor cells travel to the ovary and establish tumors there. The role of intra-ovarian microenvironment in ovarian tumor development and progression is still unclear. Our study focuses on understanding the process of extra-ovarian malignant cells migrating toward the ovary and the unique factors in the ovary that may facilitate the establishment of tumors.

Using the described animal model, we were able to recreate different stages of ovarian cancer development. To our knowledge this is the first model that closely recapitulates the early stage of ovarian cancer (Stage I) wherein the ectopically introduced ovarian cancer cells are confined in the mouse ovarian stroma and covered by the intact ovarian surface epithelium. In fact, in our model tumors found



in the ovaries were always encapsulated by the ovarian surface epithelium, which is very similar to early stage human ovarian cancer. This observation led us to the postulation that the human tumors that are diagnosed as ovarian carcinoma *in situ* can arise from extra-ovarian origins. And the extra-ovarian cancer precursors need to undergo a process of migration and implantation to home in the ovary.

Mouse models help us better understand the development of human ovarian cancers. However, it is important for us to consider their differences. For instance, unlike the human ovary, the mouse ovary is surrounded by a thin membrane called bursa. In most xenograft ovarian cancer models, cancer cells must be injected or implanted under the bursa to form tumors in the ovary³⁴. In our models, the injections did not rupture ovarian bursa. When we examined the histology of the mouse ovarian tumors, we did not observe any damage in the ovarian bursa. Even when the tumors were large the ovaries were still covered by intact bursa. Therefore, it is intriguing that the *i.p.* or intrauterine injection of OTICs formed tumors inside the ovaries. This observation indicates that the signals originated from the ovaries are able to induce a specific migratory process that includes the invasion through the ovarian bursa. Another question regarding the animal model is whether the formation of ovarian tumor was promoted by superovulation or by PMS (pregnant mares' serum) and HCG (human chorionic gonadotropin), the hormones that were injected to induce superovulation. One could argue that the hormones may affect the OTICs and possibly make them more aggressive. To exclude this possibility, we treated the OTICs with PMS and HCG *in vitro*. We did not detect any changes in their morphology, proliferation, or gene expression (data not shown).

The cells that we used in this study, OTICs, were isolated from human high grade serous ovarian carcinoma³⁵. Their molecular and cellular characteristics have been studied in depth by our group^{13,35–43}. They have shown robust tumor forming capacity and cancer stem cell-like properties. Although the OTICs used in this study might not be the actual ovarian cancer precursors, they provide us a very useful tool to study the tumor development in the ovary. One of their features is the expression of CXCR4, which is often expressed by normal and cancer stem/progenitor cells. Our data suggest that the interaction of CXCR4 and its ligand SDF-1 plays a critical role in tumor development within the ovary.

We identified SDF-1 as a main chemoattractant that recruits extraovarian malignant cells to the ovary. The chemotactic function of SDF-1/CXCR4 signaling is crucial for the recruitment and colonization of the gonads by primordial germ cells during development⁴⁴. In the mature ovary, SDF-1 regulates folliculogenesis. SDF-1/CXCR4 signaling plays an important role in maintaining the size and longevity of the primordial follicle pool⁴⁵. SDF-1 acts in concert with leptin to modulate follicular development by regulating angiogenic factors⁴⁶. The fact that SDF-1 concentration is high in the follicular fluid during ovulation and in the corpus luteum supports our hypothesis that ovulation promotes the recruitment of cancer cells to the ovary. Moreover, our data suggest that other ovulation-associated factors, such as TNF α , can enhance the SDF-1 dependent chemoattraction of cancer cells. This finding indicates that the recruitment of cancer cells to the ovary may involve multiple molecules and cell signaling networks. Understanding the mechanism of these signaling networks will lead us to discover molecules and pathways that can be targeted to lower the risk of ovarian cancer.

Our data revealed that follicle rupture and the exposure of ovarian stroma can promote the adhesion of cancer cells to the ovary. Ovulatory wound allows the entry of the cancer cells into the ovary. We demonstrated with *in vitro* models that the ruptured epithelium exposes the ECM secreted by stromal cells, which provides a collagen IV-enriched optimum scaffold supporting the adhesion of malignant cells. With the *ex vivo* model, we showed that the cancer cells spe-

cifically adhered to the areas of ruptured follicles. When we blocked SDF-1 signal, the adhesion was inhibited. Without injecting HCG to trigger the rupture of follicles, we observed the decreased number of adhesion sites. Our results indicate that blocking the SDF-1 chemoattraction or the wounding of ovarian surface epithelium may prevent the extra-ovarian malignant cells from migrating and adhering to the ovary.

In conclusion, we provide evidence that during ovulation the ovary can attract extra-ovarian malignant cells and provide a fertile soil to support the adhesion of malignant cells. Our model also allows us to further investigate the molecular mechanisms involved in the process of recruitment, establishment and progression of ovarian tumors. In the ongoing study, we try to determine the requisite phenotype that allows the extra-ovarian cancer precursors to migrate and form tumors in the ovary. We also try to understand how ovarian microenvironment completes the transformation of cancer precursors or pre-malignant cells and which factors in the ovary trigger the progression of ovarian tumors. Understanding the molecular mechanisms will aid the discovery of early detection markers and improve prevention strategies of ovarian cancer.

Methods

Chemicals and cell lines. Antibodies were purchased from Cell Signaling Technologies (Danvers, MA). SDF-1 and TNF α were from PeproTech (Rocky Hill, NJ). AMD3100 and Collagen IV from EMD Millipore (Billerica, MA). PMS and HCG were purchased from SIGMA (St. Louis, MO). OTIC and non-OTIC cell lines were established and labeled with mCherry or GFP-expressing lentivirus as previously described^{13,47}. They were cultured in RPMI1640 medium (Gibco Life technologies, Grand Island, NY) supplemented with 10% FBS. KGN cells were maintained in DMEM/F12 medium (Gibco Life technologies) with 10% FBS. Mouse ovarian surface epithelial (mOSE) cells were isolated as previously described⁴⁸ and cultured in 199/105 medium (Gibco Life technologies) with 10% FBS. After mOSE cells were isolated the rest of the mouse ovaries were further dissociated with trypsin (Gibco Life technologies) to isolate the mouse ovarian stromal (mOST) cells. mOST cells were cultured in DMEM medium with 10% FBS. Human OSE and OST cells were isolated from healthy ovarian tissue specimens and cultured in 199/105 medium with 10% FBS.

Mouse models. All experiments were performed in accordance with the relevant guidelines and regulations that were approved by the Institutional Animal Care and Use Committee at Yale University. Six-week-old female athymic nude mice were purchased from Harlan Sprague Dawley Inc. (Indianapolis, IN). The animals were maintained under pathogen-free conditions, and food and water were supplied *ad libitum*. Mice were ear-tagged and followed individually throughout the study. Mice were anesthetized by gas anesthesia (3% isoflurane) prior to injection or imaging. In the interperitoneal injection model, 7×10^6 cells (in 300 μ l of RPMI-1640 medium) were injected into mice. In the intrauterine and injection model, 2×10^6 cells (in 50 μ l of RPMI-1640 medium) were injected into one side uterine horn by surgery. Superovulation was induced by interperitoneally injecting 5 IU PMS and 48 hours later 5 IU HCG. Cancer cells were injected 24 hours after PMS injection. Tumors were monitored by red fluorescence and, concurrently, X-ray images with the Bruker In-Vivo MS FX PRO Imaging System (Billerica, MA).

Immunostaining. Immunohistochemistry staining was performed as previously described³⁷. Immunohistochemistry staining was performed as previously described⁴⁹. Antibodies were diluted as following: SDF-1 (1 : 100), CK8 (1 : 200) and vimentin (1 : 100).

Quantitative real-time PCR. Total RNA was extracted from cells or tumor tissues using RNeasy Mini Kit (Qiagen, Austin, Texas) according to the manufacturer's instruction. cDNA was synthesized from total RNA (1 μ g) with Verso cDNA Kit (Thermo Scientific, Waltham, Massachusetts) according to the manufacturer's instruction. Quantification of mRNA was performed using KAPA SYBR FAST qPCR Kit (KAPA Biosystems, Woburn, Massachusetts) followed by detection with the CFX96TM PCR detection system (Bio-Rad). GAPDH was used as reference gene for normalization. Relative expression was calculated using the comparative $\Delta\Delta$ CT method and the change in mRNA expression was calculated as fold change. All reactions were performed in triplicate. Primer sequences are listed in the supplementary information.

Western blot. Cells were washed twice with ice-cold PBS and cell lysates were prepared with KLB buffer (1% Triton X-100, 0.05% SDS, 100 mM Na₂HPO₄, and 150 mM NaCl). Then, 20 μ g of each protein lysate were electrophoresed on a 12% SDS-polyacrylamide gel. The proteins were transferred onto Immobilon-P PVDF membranes (Millipore). After blocking with PBS-0.05% Tween 20 and 5% milk, the membranes were probed with primary antibodies at 4°C overnight. They were diluted as following: anti-ERK (1 : 1000), anti-pERK (1 : 1000), GAPDH (1 : 10000). After washing with PBS-Tween, the membranes were incubated with peroxidase-conjugated anti-rabbit (1 : 10000) or anti-mouse (1 : 10000) secondary antibody



(Dako, Denmark) in 5% non-fat milk. The blots were developed using the enhanced chemiluminescence (ECL) system (NEN Life Sciences, Waltham, MA) and imaged using the Kodak 2000MM Image Station.

Migration assay. Migration assay was performed as previously described⁵⁰. Condition medium was collected from KGN cells cultured in Opti MEM medium for 48 hours and placed at the lower chamber. mCherry-OTICs were seeded in the upper chamber. After 24 hours, the cells that migrated to the lower chamber were counted.

Flowcytometry. The non-treated and 10 ng/ml TNF α -treated OTICs were suspended in PBS, 0.5% BSA and stained with anti-CXCR4 antibody for 30 min at 4°C. After washing with PBS, cells were incubated with Alexa Fluor 594 anti-rabbit antibody for 30 min at 4°C. Fluorescence-activated cell sorting and analysis were performed on a BD Special Order FACS Aria II system and Diva v6.1.1 (BD Biosciences, San Jose, California). Live single cells were gated based on scatter properties and analyzed for their surface CXCR4 expression.

Wound healing assay. Migration assay was performed as previously described⁴². During the assay, OTICs were treated with 100 ng/ml SDF-1 or first pre-treated with 10 ng/ml TNF α for 2 hours and then co-treated with SDF-1 and TNF α .

Adhesion assay. In the adhesion assay, fluorescent OTICs were seeded on the top of the monolayer cells, the extracted ECM, or Collagen IV coated surface. mOSE or mOST cells were cultured for 48 hours to form the confluent cell monolayer. Cell-derived ECM or collagen IV coated surface was prepared as previously described⁵¹.

Ex vivo adhesion assay. Ovaries were collected from mice after superovulation was induced. Fat and connective tissues were trimmed off to clean the ovaries. Each ovary was co-cultured with 10⁶ mCherry-OTICs in a 15 ml tube with 3 ml RPMI1640 medium. The tubes were incubated in a shaker at 37°C. After 24 hours, the ovaries were washed with PBS twice and then examined under Modular Routine Fluorescent Stereo Microscope M80 (Leica, Germany).

- Siegel, R., Ma, J., Zou, Z. & Jemal, A. Cancer statistics, 2014. *CA Cancer J Clin* **64**, 9–29 (2014).
- Lee, Y. *et al.* A candidate precursor to serous carcinoma that originates in the distal fallopian tube. *J Pathol* **211**, 26–35 (2007).
- Leonhardt, K., Eienkel, J., Sohr, S., Engeland, K. & Horn, L. C. p53 signature and serous tubal in-situ carcinoma in cases of primary tubal and peritoneal carcinomas and serous borderline tumors of the ovary. *Int J Gynecol Pathol* **30**, 417–24 (2011).
- Norquist, B. M. *et al.* The molecular pathogenesis of hereditary ovarian carcinoma: alterations in the tubal epithelium of women with BRCA1 and BRCA2 mutations. *Cancer* **116**, 5261–71 (2010).
- Folkins, A. K. *et al.* A candidate precursor to pelvic serous cancer (p53 signature) and its prevalence in ovaries and fallopian tubes from women with BRCA mutations. *Gynecol Oncol* **109**, 168–73 (2008).
- Marquez, R. T. *et al.* Patterns of gene expression in different histotypes of epithelial ovarian cancer correlate with those in normal fallopian tube, endometrium, and colon. *Clin Cancer Res* **11**, 6116–26 (2005).
- Khunamornpong, S., Suprasert, P., Chiangmai, W. N. & Siriaunkgul, S. Metastatic tumors to the ovaries: a study of 170 cases in northern Thailand. *Int J Gynecol Cancer* **16 Suppl 1**, 132–8 (2006).
- Lee, K. R. & Nucci, M. R. Ovarian mucinous and mixed epithelial carcinomas of mullerian (endocervical-like) type: a clinicopathologic analysis of four cases of an uncommon variant associated with endometriosis. *Int J Gynecol Pathol* **22**, 42–51 (2003).
- Kamran, M. W. *et al.* Opportunistic and interventional salpingectomy in women at risk: a strategy for preventing pelvic serous cancer (PSC). *Eur J Obstet Gynecol Reprod Biol* **170**, 251–4 (2013).
- Richards, J. S., Russell, D. L., Ochsner, S. & Espey, L. L. Ovulation: new dimensions and new regulators of the inflammatory-like response. *Annu Rev Physiol* **64**, 69–92 (2002).
- Purdie, D. M., Bain, C. J., Siskind, V., Webb, P. M. & Green, A. C. Ovulation and risk of epithelial ovarian cancer. *Int J Cancer* **104**, 228–32 (2003).
- Tung, K. H. *et al.* Effect of anovulation factors on pre- and postmenopausal ovarian cancer risk: revisiting the incessant ovulation hypothesis. *Am J Epidemiol* **161**, 321–9 (2005).
- Craveiro, V. *et al.* Phenotypic modifications in ovarian cancer stem cells following Paclitaxel treatment. *Cancer Med* **2**, 751–62 (2013).
- Machelon, V. & Emilie, D. Production of ovarian cytokines and their role in ovulation in the mammalian ovary. *Eur Cytokine Netw* **8**, 137–43 (1997).
- Zuccarello, D. *et al.* How the human spermatozoa sense the oocyte: a new role of SDF1-CXCR4 signalling. *Int J Androl* **34**, e554–65 (2011).
- Ratajczak, M. Z. *et al.* A novel perspective on stem cell homing and mobilization: review on bioactive lipids as potent chemoattractants and cationic peptides as underappreciated modulators of responsiveness to SDF-1 gradients. *Leukemia* **26**, 63–72 (2012).
- Greenbaum, A. *et al.* CXCL12 in early mesenchymal progenitors is required for haematopoietic stem-cell maintenance. *Nature* **495**, 227–30 (2013).
- Barbolina, M. V. *et al.* Microenvironmental regulation of chemokine (C-X-C-motif) receptor 4 in ovarian carcinoma. *Mol Cancer Res* **8**, 653–64 (2010).
- Popple, A. *et al.* The chemokine, CXCL12, is an independent predictor of poor survival in ovarian cancer. *Br J Cancer* **106**, 1306–13 (2012).
- Nishi, Y. *et al.* Establishment and characterization of a steroidogenic human granulosa-like tumor cell line, KGN, that expresses functional follicle-stimulating hormone receptor. *Endocrinology* **142**, 437–45 (2001).
- Wojcechowskyj, J. A., Lee, J. Y., Seeholzer, S. H. & Doms, R. W. Quantitative phosphoproteomics of CXCL12 (SDF-1) signaling. *PLoS One* **6**, e24918 (2011).
- Hunt, J. S. Expression and regulation of the tumour necrosis factor- α gene in the female reproductive tract. *Reprod Fertil Dev* **5**, 141–53 (1993).
- Murdoch, W. J., Colgin, D. C. & Ellis, J. A. Role of tumor necrosis factor- α in the ovulatory mechanism of ewes. *J Anim Sci* **75**, 1601–5 (1997).
- Rodgers, R. J. & Irving-Rodgers, H. F. The roles of the ovarian extracellular matrix in fertility. *Soc Reprod Fertil Suppl* **67**, 217–30 (2010).
- Rodgers, R. J., Irving-Rodgers, H. F. & Russell, D. L. Extracellular matrix of the developing ovarian follicle. *Reproduction* **126**, 415–24 (2003).
- Carmeliet, G., Himpens, B. & Cassiman, J. J. Selective increase in the binding of the alpha 1 beta 1 integrin for collagen type IV during neurite outgrowth of human neuroblastoma TR 14 cells. *J Cell Sci* **107 (Pt 12)**, 3379–92 (1994).
- Katoh, D. *et al.* Binding of alphavbeta1 and alphavbeta6 integrins to tenascin-C induces epithelial-mesenchymal transition-like change of breast cancer cells. *Oncogenesis* **2**, e65 (2013).
- Tuckwell, D. & Humphries, M. Integrin-collagen binding. *Seminars in Cell & Developmental Biology* **7**, 649–657 (1996).
- Crum, C. P. *et al.* The distal fallopian tube: a new model for pelvic serous carcinogenesis. *Curr Opin Obstet Gynecol* **19**, 3–9 (2007).
- Crum, C. P. *et al.* Through the glass darkly: intraepithelial neoplasia, top-down differentiation, and the road to ovarian cancer. *J Pathol* **231**, 402–12 (2013).
- Crum, C. P., McKeon, F. D. & Xian, W. BRCA, the oviduct, and the space and time continuum of pelvic serous carcinogenesis. *Int J Gynecol Cancer* **22 Suppl 1**, S29–34 (2012).
- Kim, J. *et al.* High-grade serous ovarian cancer arises from fallopian tube in a mouse model. *Proc Natl Acad Sci U S A* **109**, 3921–6 (2012).
- Perets, R. *et al.* Transformation of the fallopian tube secretory epithelium leads to high-grade serous ovarian cancer in Brca; Tp53; Pten models. *Cancer Cell* **24**, 751–65 (2013).
- Sale, S. & Orsulic, S. Models of ovarian cancer metastasis: Murine models. *Drug Discov Today Dis Models* **3**, 149–154 (2006).
- Alvero, A. B. *et al.* Molecular phenotyping of human ovarian cancer stem cells unravels the mechanisms for repair and chemoresistance. *Cell Cycle* **8**, 158–66 (2009).
- Chen, R. *et al.* Regulation of IKKbeta by miR-199a affects NF-kappaB activity in ovarian cancer cells. *Oncogene* **27**, 4712–23 (2008).
- Alvero, A. B. *et al.* Stem-like ovarian cancer cells can serve as tumor vascular progenitors. *Stem Cells* **27**, 2405–13 (2009).
- Yin, G. *et al.* TWISTING stemness, inflammation and proliferation of epithelial ovarian cancer cells through MIR199A2/214. *Oncogene* **29**, 3545–53 (2010).
- Alvero, A. B. *et al.* Targeting the mitochondria activates two independent cell death pathways in ovarian cancer stem cells. *Mol Cancer Ther* **10**, 1385–93 (2011).
- Chefetz, I., Holmberg, J. C., Alvero, A. B., Visintin, I. & Mor, G. Inhibition of Aurora-A kinase induces cell cycle arrest in epithelial ovarian cancer stem cells by affecting NFkB pathway. *Cell Cycle* **10**, 2206–14 (2011).
- Alvero, A. B., Montagna, M. K., Craveiro, V., Liu, L. & Mor, G. Distinct subpopulations of epithelial ovarian cancer cells can differentially induce macrophages and T regulatory cells toward a pro-tumor phenotype. *Am J Reprod Immunol* **67**, 256–65 (2012).
- Chefetz, I. *et al.* TLR2 enhances ovarian cancer stem cell self-renewal and promotes tumor repair and recurrence. *Cell Cycle* **12**, 511–21 (2013).
- Yin, G. *et al.* Constitutive proteasomal degradation of TWIST-1 in epithelial-ovarian cancer stem cells impacts differentiation and metastatic potential. *Oncogene* **32**, 39–49 (2013).
- Ara, T. *et al.* Impaired colonization of the gonads by primordial germ cells in mice lacking a chemokine, stromal cell-derived factor-1 (SDF-1). *Proc Natl Acad Sci U S A* **100**, 5319–23 (2003).
- Holt, J. E. *et al.* CXCR4/SDF1 interaction inhibits the primordial to primary follicle transition in the neonatal mouse ovary. *Dev Biol* **293**, 449–60 (2006).
- Park, M. J. *et al.* Expression of SDF-1alpha and leptin, and their effect on expression of angiogenic factors in mouse ovaries. *Clin Exp Reprod Med* **38**, 135–41 (2011).
- Kamsteeg, M. *et al.* Phenoxodiol--an isoflavone analog--induces apoptosis in chemoresistant ovarian cancer cells. *Oncogene* **22**, 2611–20 (2003).
- Roby, K. F. *et al.* Development of a syngeneic mouse model for events related to ovarian cancer. *Carcinogenesis* **21**, 585–91 (2000).
- Xia, X. *et al.* Fluorescence in situ hybridization using an old world monkey Y chromosome specific probe combined with immunofluorescence staining on rhesus monkey tissues. *J Histochem Cytochem* **55**, 1115–21 (2007).
- Abrahams, V. M. *et al.* A role for TLRs in the regulation of immune cell migration by first trimester trophoblast cells. *J Immunol* **175**, 8096–104 (2005).



51. Bass, M. D. *et al.* Syndecan-4-dependent Rac1 regulation determines directional migration in response to the extracellular matrix. *J Cell Biol* **177**, 527–38 (2007).

Acknowledgments

This study was supported in part by NIH gGrant RO1CA127913, the Sands Family Foundation, the Debra Levin Endowment Fund, and the Discovery to Cure Program.

Author contributions

Y.Y.-H. conducted experiments, developed the hypothesis, analyzed the data, coordinated the project and wrote the manuscript. M.G.-S., conducted experiments, analyzed and interpreted the data. N.S., W.D.J., J.C.H. and V.C. conducted mouse experiments. A.B.A. discussed the data and contributed to manuscript preparation. G.M. conceived and led the project, interpreted the data and revised the manuscript.

Additional information

Supplementary information accompanies this paper at <http://www.nature.com/scientificreports>

Competing financial interests: The authors declare no competing financial interests.

How to cite this article: Yang-Hartwich, Y. *et al.* Ovulation and extra-ovarian origin of ovarian cancer. *Sci. Rep.* **4**, 6116; DOI:10.1038/srep06116 (2014).



This work is licensed under a Creative Commons Attribution-NonCommercial-NoDerivs 4.0 International License. The images or other third party material in this article are included in the article's Creative Commons license, unless indicated otherwise in the credit line; if the material is not included under the Creative Commons license, users will need to obtain permission from the license holder in order to reproduce the material. To view a copy of this license, visit <http://creativecommons.org/licenses/by-nc-nd/4.0/>